

# Design Optimization of Motor/Generator Full-load Characteristics in Two-mode Hybrid Vehicles

Kukhyun Ahn and Panos Y. Papalambros

University of Michigan-Ann Arbor

Copyright © 2009 SAE International

## ABSTRACT

An important benefit in adopting multi-mode hybrid powertrains is the possibility of downsizing the electric motor/generator (M/G) units. This paper discusses design optimization of M/G full-load operation envelopes. A three-dimensional operation space analysis is introduced and the full-load speed-torque envelopes of M/G units appear as constraints in the powertrain operation space. The analysis shows how the change in the M/G characteristics affects the powertrain full-load performance and how the M/G units can be downsized by combining multiple modes. When the acceleration performance of a two-mode hybrid vehicle is estimated using this analysis method, the trade-off between enhancing performance and reducing M/G full-load capacities is formulated as an optimization problem. The results show significant improvement in dynamic performance at reduced M/G cost.

## INTRODUCTION

Power-split hybrid electric vehicles (HEVs) have been the most successful configurations since their pioneering debut in the marketplace. However, relatively low highway fuel efficiency and high manufacturing costs are drawbacks for this configuration. In an effort to overcome these deficiencies, manufacturers have developed advanced versions of the power-split HEV, referred to as multi-mode hybrid systems.

The multi-mode hybrid systems combine more than one power-split operation mode. For example, a system can use both input-split and compound-split modes; it can have additional parallel hybrid operation options, engineered to improve acceleration and cruise

performance. These systems also aim at improving fuel efficiency and reducing manufacturing costs. According to the previous research on the merits of these systems, the improvements in dynamic performance and the effects of M/G downsizing look far more promising than the increase in fuel efficiency [1, 2]. In particular, the requirements for M/G units may be greatly decreased, resulting in lower weight and cost.

This paper investigates these potential benefits of a two-mode hybrid system by focusing on the effects of the M/G full-load characteristics on the vehicle acceleration performance. To this end, two optimization frameworks are developed for powertrain operation and for component characteristics design, which will later be integrated in one problem.

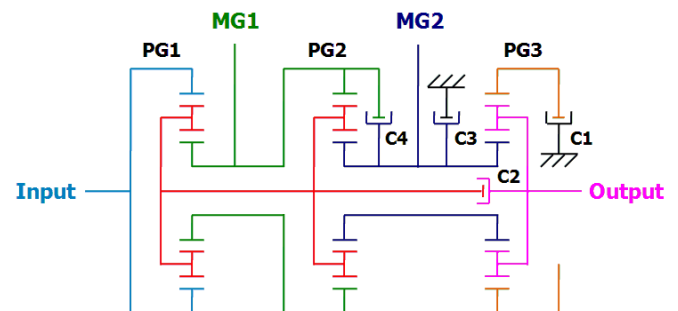


Fig. 1: Schematic of the two-mode hybrid powertrain

## SYSTEM DESCRIPTION

A patented two-mode hybrid powertrain with fixed-gear options will be investigated in the analyses to follow [3]. Its schematic view is shown in Fig. 1. It uses three

The Engineering Meetings Board has approved this paper for publication. It has successfully completed SAE's peer review process under the supervision of the session organizer. This process requires a minimum of three (3) reviews by industry experts.

All rights reserved. No part of this publication may be reproduced, stored in a retrieval system, or transmitted, in any form or by any means, electronic, mechanical, photocopying, recording, or otherwise, without the prior written permission of SAE.

ISSN 0148-7191

Positions and opinions advanced in this paper are those of the author(s) and not necessarily those of SAE. The author is solely responsible for the content of the paper.

**SAE Customer Service:** Tel: 877-606-7323 (inside USA and Canada)  
Tel: 724-776-4970 (outside USA)  
Fax: 724-776-0790  
Email: [CustomerService@sae.org](mailto:CustomerService@sae.org)

**SAE Web Address:** <http://www.sae.org>

Printed in USA

**SAE** International

planetary gear sets (PG1, PG2, and PG3) and four wet clutches (C1 through C4) to allow for six different operation modes: two electrically variable transmission (EVT) modes and four fixed-gear (FG) modes. Clutch operations and quasi-static equations of motion for each mode of the system have been detailed in the literature [1, 4, 5]. Here, a brief description of the system and generalized representations of the equations of motion are presented for facilitate the discussions in the following sections.

When only C1 is engaged, the transmission functions as an input-split device (EVT1), and PG3 acts merely as a single-ratio reduction gear. During this operation, C4 can be engaged to realize a parallel hybrid mechanism (FG1). As the vehicle velocity increases, the powertrain shifts modes from EVT1 to EVT2, which is a compound-split mode. FG2 is an inherent mode between the two EVT modes, and enables the synchronous shift. During this shift, C2 is engaged and C1 is released, minimizing a possible shock. In this mode, the ring gear of PG3 is free-wheeling, functioning neither as a power-split device nor as a single-ratio gear. The other two fixed-gear modes will not be discussed in this paper. (See references [1, 4, 5] for further details.)

Before presenting the generalized quasi-static equations of motion, the generalized representation of the power-split system is introduced [4, 6]. The lever diagram in Fig. 2 visualizes the relationships among elements by interpreting the rotational motions into linear ones. The representation can comprise all three power-split cases. The lever lengths,  $\alpha$  and  $\beta$ , are the distances from the output to M/G units when the lever length of the input is normalized to 1.

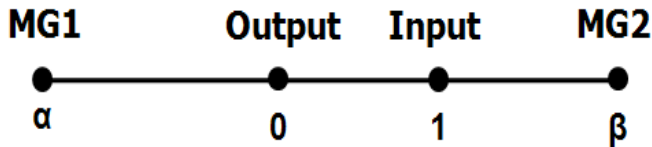


Fig. 2: Combined lever diagram

Using this representation, speeds and torques of M/G units are expressed with respect to those of the input and output in Table 1. In the case of EVT1, the output speed in the equations is not identical but proportional to the actual output speed by the reduction ratio of PG3. For FG modes, another set of generalized equations are given. There are four equations with respect to the eight component state variables in both cases. The last equation shared by EVT and FG modes is the generalized power conversion equation, which takes the inverse of the M/G conversion efficiency when the M/G works as a generator or the M/G power is negative. The generalized lever lengths for the two EVT modes, the reduction ratio for EVT1 mode, and the coefficients in the FG equations are given in Equations (1) to (6).

Table 1: Generalized quasi-static equations of motion

	<i>EVT</i>	<i>FG</i>
<i>Speed</i>	$\omega_1 = \alpha\omega_i + (1-\alpha)\omega_o$ $\omega_2 = \beta\omega_i + (1-\beta)\omega_o$	$\omega_i = k_i\omega_o$ $\omega_1 = k_1\omega_o$ $\omega_2 = k_2\omega_o$
<i>Torque</i>	$T_1 = \frac{1-\beta}{\beta-\alpha}T_i + \frac{\beta}{\beta-\alpha}T_o$ $T_2 = \frac{1-\alpha}{\alpha-\beta}T_i + \frac{\alpha}{\alpha-\beta}T_o$	$T_o = k_iT_i + k_1T_1 + k_2T_2$
<i>Power Conversion</i>	$P_b = \frac{\omega_1 T_1}{\eta_1(\omega_1, T_1)} + \frac{\omega_2 T_2}{\eta_2(\omega_2, T_2)}$	

$$\text{EVT1: } \alpha = \frac{1+r_2}{1-r_1r_2}, \quad \beta = 0, \quad \rho = \frac{1+r_3}{r_3} \quad (1)$$

$$\text{EVT2: } \alpha = -\frac{1}{r_1}, \quad \beta = \frac{1}{r_1r_2} \quad (2)$$

$$\text{FG1: } k_i = \frac{1+r_3}{r_3}, \quad k_1 = \frac{1+r_3}{r_3}, \quad k_2 = \frac{1+r_3}{r_3} \quad (3)$$

$$\text{FG2: } k_i = \frac{r_1r_2+r_3}{r_3}, \quad k_1 = \frac{r_3-r_2}{r_3}, \quad k_2 = \frac{1+r_3}{r_3} \quad (4)$$

$$\text{FG3: } k_i = 1, \quad k_1 = 1, \quad k_2 = 1 \quad (5)$$

$$\text{FG4: } k_i = 1-r_1r_2, \quad k_1 = 1+r_2, \quad k_2 = 0 \quad (6)$$

Here,  $P$ ,  $T$ , and  $\omega$  denote power (W), torque (Nm), and speed (rad/s) of each component, respectively, and  $\eta$  is the M/G conversion efficiency.  $\alpha$  and  $\beta$  are the normalized locations of M/G units, and  $r_1$ ,  $r_2$ , and  $r_3$  are the planetary gear ratios of PG1, PG2, and PG3.  $\rho$  is the reduction ratio of PG3 in EVT1 mode, and  $k$  is the component speed ratio to the output in FG modes. 1, 2,  $i$ ,  $o$ , and  $b$  are the subscripts for M/G1, M/G2, input, output, and battery, respectively.

## POWERTRAIN FULL-LOAD OPERATION

The powertrain needs to be operated in such a way that the output shaft can transmit the maximum torque from the powertrain to the final drive. This can be regarded as an optimization problem, and is solved for the corresponding vehicle velocity. This optimization problem, however, is far more complicated than in conventional vehicles, where the engine exerts its wide-

open-throttle torque while the engine speed is determined by the vehicle velocity and transmission ratio. In two-mode hybrid powertrains, each mode has three degrees of freedom to determine the output torque, and each power component should be operated within its feasible operation domain or the full-load envelope. This can be formulated as either of two optimization problems depending on whether the operation is in EVT or FG mode. See Table 2.

The three independent operation variables are engine speed, engine torque, and M/G2 torque in the case of EVT modes, and engine, M/G1, and M/G2 torques for FG modes. The problem will be solved repeatedly, possibly several hundreds of times, along an output speed grid ranging from 0 to its maximum. The two cases will share the constraints on the component speeds, torques, and power, which will produce fairly different shapes in the respective three-dimensional design spaces.

Table 2: Optimization statements

	<i>EVT</i>	<i>FG</i>
<i>Minimize</i>	$\frac{1-\alpha}{\alpha} T_i + \frac{\beta-\alpha}{\alpha} T_2$	$-k_i T_i - k_1 T_1 - k_2 T_2$
<i>With respect to</i>	$\omega_i, T_i, T_2$	$T_i, T_1, T_2$
<i>Subject to</i>	$\omega_{i,\min} \leq \omega_i \leq \omega_{i,\max}$ $0 \leq T_i \leq T_{i,\max}(\omega_i)$ $\omega_{1,\min} \leq \omega_1 \leq \omega_{1,\max}$ $T_{1,\min}(\omega_1) \leq T_1 \leq T_{1,\max}(\omega_1)$ $\omega_{2,\min} \leq \omega_2 \leq \omega_{2,\max}$ $T_{2,\min}(\omega_2) \leq T_2 \leq T_{2,\max}(\omega_2)$ $P_{b,\min} \leq P_b \leq P_{b,\max}$	

## DESIGN SPACE ANALYSIS

The optimization problems described in the previous section do not have as large a design space as other power management problems with tens or hundreds of variables. Furthermore, the problem size can be reduced further by applying dominance and monotonicity analysis in some of the cases. This kind of analysis of the design space will give us a better understanding of the relations and interactions among the components. Here, we analyze the three-dimensional design space of the operation in EVT2 mode, which is a compound-split mode and has the most complicated and nonlinear design space. The analysis in this section is presented with a given powertrain design, which is the result of the powertrain design optimization problem in the Results section. (See Table 4.)

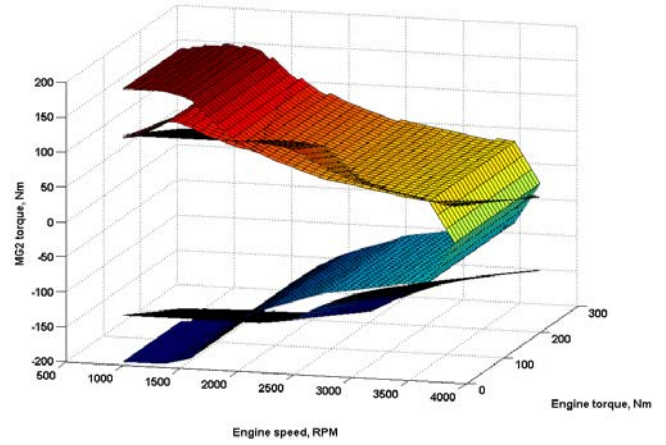


Fig. 3: Constraint surfaces in the design space

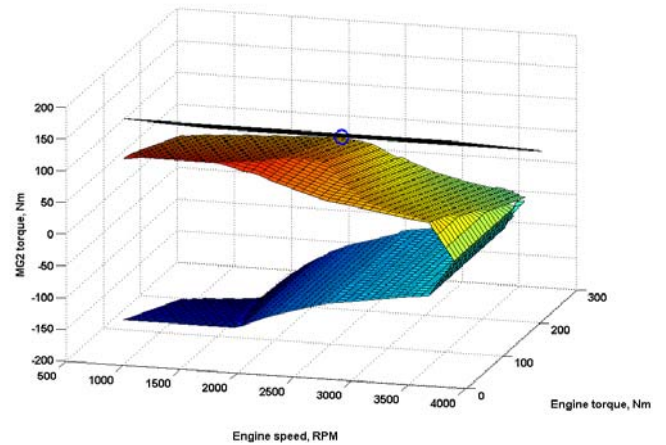


Fig. 4: Feasible domain and constant objective plane

Fig. 3 shows how some of the constraints appear in the design space. The plots are for a specific output speed (100 rad/s), and entirely different design space shapes can be observed for different output speeds. The upper three surfaces are the inequality constraints on M/G1 torque, M/G2 torque, and battery power, respectively. The lower two surfaces are derived from the other inequalities, but the constraint on minimum battery power does not appear because it is dominated by the others. The simple bound constraints would appear as vertical surfaces and are omitted for clarity.

The intersection set of all the constraints will form the feasible domain, which is shown in Fig. 4, together with a constant objective plane. As illustrated in the figure, the optimal solution will be found at the last point of contact between the plane and the feasible domain as the plane moves along the direction of minimization. This visualization shows that the active constraints are the M/G1 and engine torque upper limits, suggesting that increasing the components' torque capacities will improve the performance, at least for the corresponding output speed. Fig. 5 shows how the M/G1 upper torque limit constrains the maximum output torque as the vehicle accelerates.

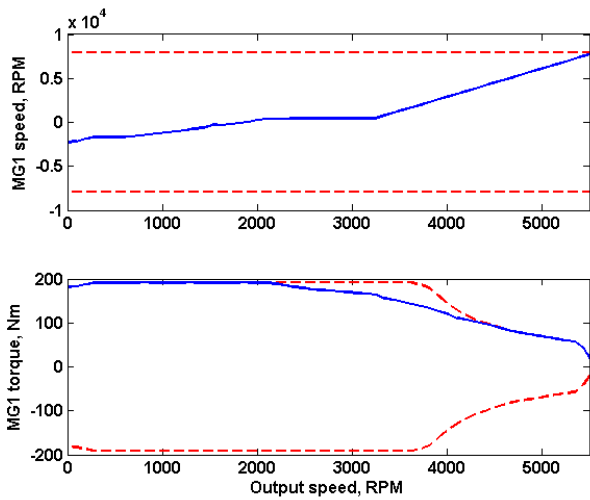


Fig. 5: Constraints on M/G1 speed and torque

The full-load torque boundary acts as an active constraint for most of the output speeds. Apparently, this component can be said to be undersized, and the system requires a higher torque M/G1 to improve the acceleration performance. This can also be viewed in a different perspective with the operation point plot in Fig. 6.

The open circles are operation points visited during the full acceleration simulation. Concentrated use can be seen in the high torque backward generation area. Fortunately, this can be avoided in an actual situation because the powertrain logic will choose to use another mode at the corresponding lower vehicle velocity region. The full-load acceleration mode shift scheme predicts the altered operation points in Fig. 7.

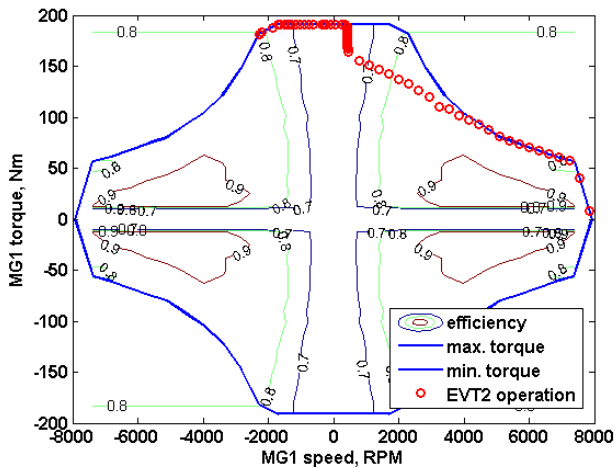


Fig. 6: M/G1 operation point during EVT2 acceleration

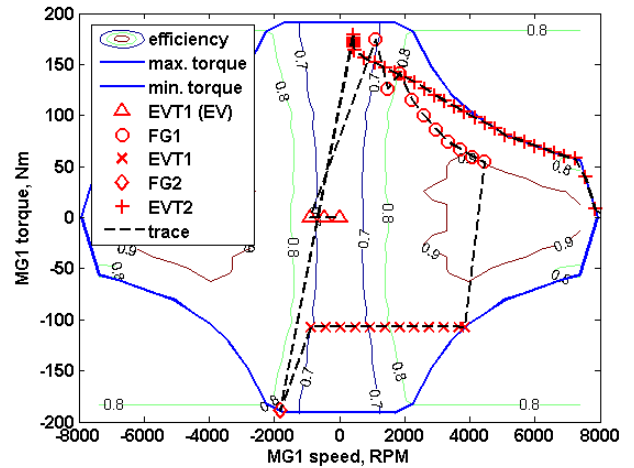


Fig. 7: M/G1 operation points during acceleration

Unlike in Fig. 6, the powertrain is operated in such a way that far fewer M/G1 operation points are on the high torque boundary. The machine does not seem to be undersized now, and this is one of the advantages that multi-mode transmissions have in reducing component required capacities.

A similar analysis can be made in regards to the M/G2 operation in EVT1 mode. At a lower vehicle velocity, the input-split powertrain cannot use the full battery power because M/G2 uses the break-down torque at low speed. High torque motors will improve the acceleration performance; however, high torque motors with high break-down torque are even more expensive than high speed motors, and the manufacturing costs will greatly increase as a result.

Fig. 8 shows a dramatic change in M/G2 operation, which results from combining multiple modes, including compound-split and fixed-gear modes. Immediately after the short pure-electric EVT1 mode, the powertrain stops operating M/G2 in the full-load torque region until it revisits EVT1 mode for a short moment. The mode used between these two EVT1 operations is FG1. (Mode shifts during acceleration will be discussed in more detail in the following section.) This also explains why the addition of this fixed-gear mode can improve the acceleration performance at lower vehicle velocities [1]. Another important thing to notice is the speed of the machine. With the use of FG2 and EVT2 modes, M/G2 does not have to cover the high speed range because it decreases the speed in FG2 and EVT2 modes. This makes it possible to use a reduction gear between M/G2 and the output shaft and multiply the M/G2 torque. These effects together greatly help to reduce the capacity of M/G2, as was the case with M/G1.

A similar visualization is presented for reference in Fig. 9 to show the operation points and constraints of the engine during acceleration.

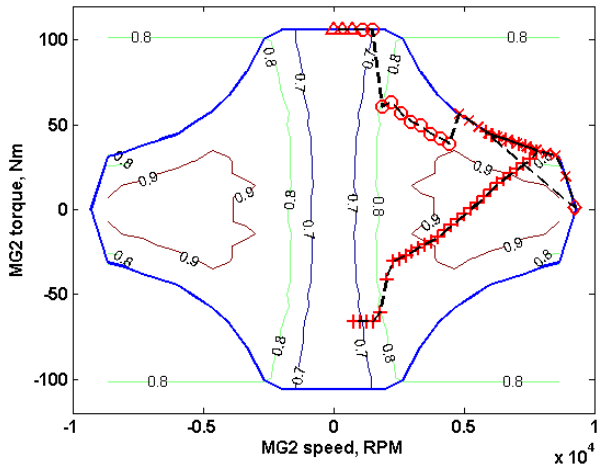


Fig. 8: M/G2 operation points during acceleration

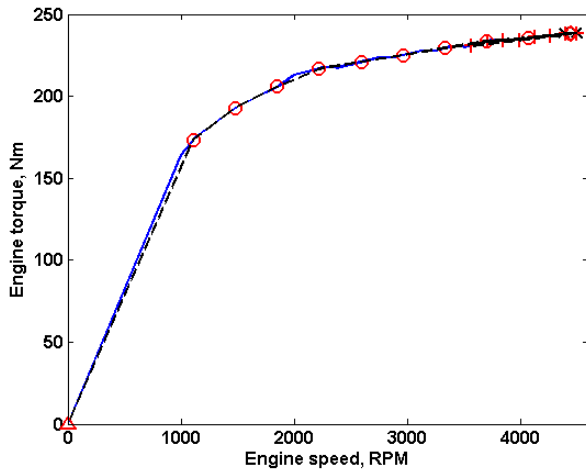


Fig. 9: Engine operation points during acceleration

### SHIFT SCHEME DURING ACCELERATION

In addition to the relatively complicated procedure detailed in the previous section, the two-mode system requires further consideration in order to find the maximum torque at a given vehicle velocity. Since there are six operation modes, they need to be compared to develop a shift scheme during acceleration. The simplest method to begin with is taking the envelope of all six maximum torque curves plotted and superposed on an output speed-torque plane. In reality, using this shift scheme will cause many problems and greatly deteriorate the ride comfort because of shocks during shifting. Thus, the scheme needs to be modified to achieve synchronous shifts.

The modified shift strategy inevitably sacrifices a certain amount of the maximum torque. For example, the powertrain needs to stop operating in EVT1 mode and switch to FG2 mode at the output speed of 2540 RPM, according to the modified scheme. (See Fig. 10.) Past that output speed, the speed of the PG2 carrier will

diverge from that of the PG3 carrier or the output speed, which are the two plate speeds of C2. Therefore, the maximum output torque of EVT1 mode above this shift point will not be used although it is greater than that of EVT2 by up to 100 Nm. With these additional considerations, the following shift scheme is developed and used in the evaluation of the acceleration performance.

At a standstill, the vehicle starts in EVT1 mode. In this first stage, however, the engine is turned off and the vehicle runs in PEV (purely electric vehicle) mode. When the M/G2 speed approaches the engine ignition speed, M/G1 is controlled to increase the engine speed to the same speed as that of M/G2. A synchronous shift occurs and the engine is turned on. This is the second stage in FG1 mode. When the engine speed reaches its maximum, C4 is disengaged, and the powertrain operates in EVT1 mode again (Stage 3). As described in the previous paragraph, the shift from EVT1 to FG2 occurs at the highest vehicle velocity where the synchronous shift is possible (Stage 4). By disengaging C1 in Stage 4, the final shift is made and the powertrain is in EVT2 mode, the last stage.

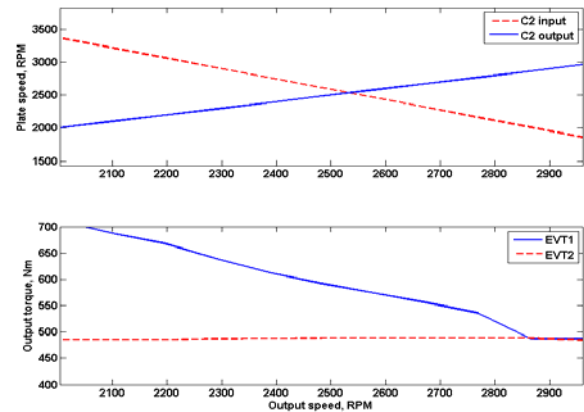


Fig. 10: Synchronous shift via FG2 mode

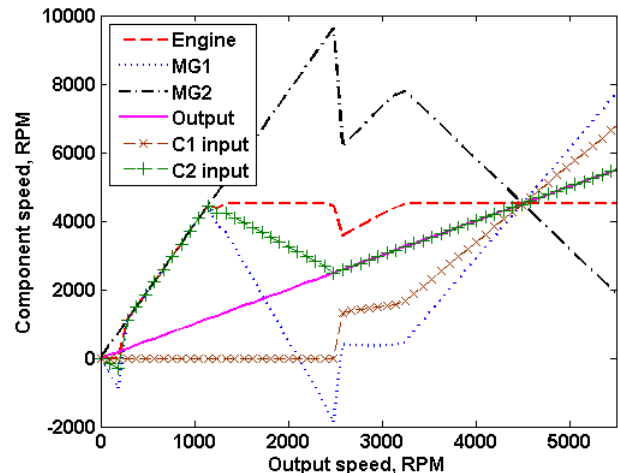


Fig. 11: Component speeds during acceleration

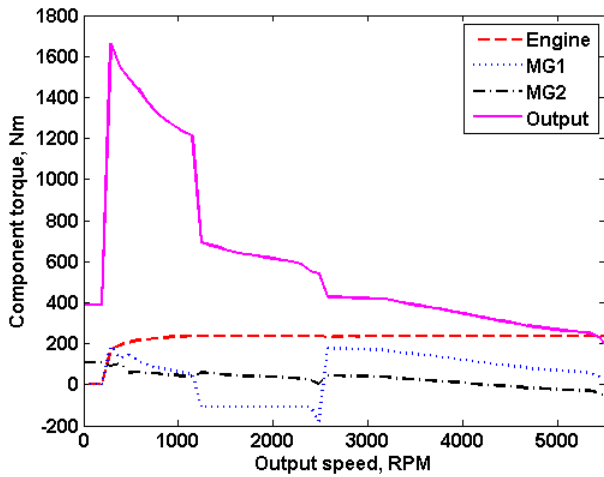


Fig. 12: Component torques during acceleration

The speeds of the components are displayed in Fig. 11 together with some clutch plate speeds. At the output speed near 2500 RPM, mode shifts were made from EVT1 via FG2 to EVT2. The speed traces of clutch plates show the input and output plates of C2 had the same speed at the moment of shifting, ensuring a synchronous shift.

The maximum powertrain torque envelope is obtained along the scheme and displayed in Fig. 12. In acceleration simulations, the performance is estimated under the assumption that the powertrain produces the maximum torque, shown in the following section.

Fig.13 shows how much electric power was used from the battery during acceleration. Certainly, the battery power limit was the active constraint most of the time, and a higher capacity will lead to better performance. However, it is more important to notice that the multi-mode powertrain can make use of the full battery power by adopting FG1 mode at lower output speeds, unlike the single-mode powertrain.

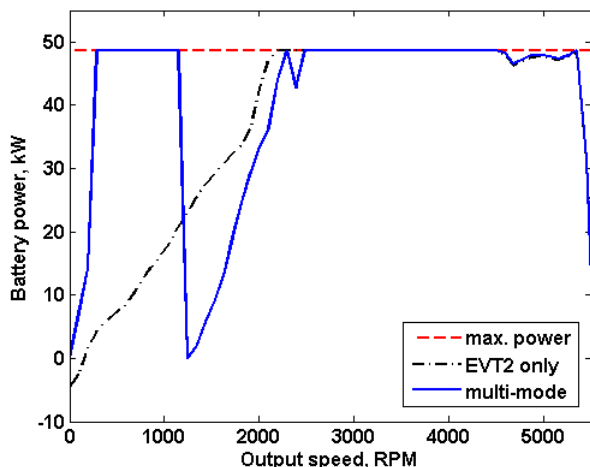


Fig. 13: Battery power use during acceleration

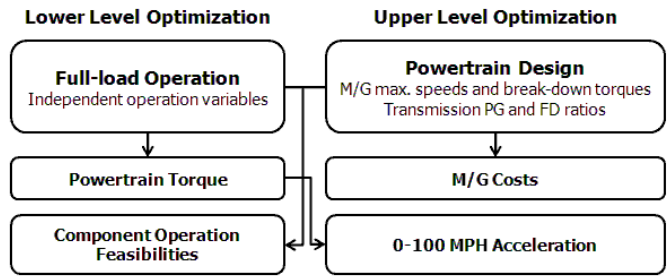


Fig. 14: Optimization framework overview

## M/G FULL-LOAD CHARACTERISTICS DESIGN

We develop an optimization framework in which the characteristics of the components can be designed. The full-load operation optimization framework and the acceleration shift scheme will be integrated in this upper level optimization problem as a nested optimization sub-problem. The flow diagram in Fig. 14 shows the overview of the framework.

The upper level problem is solved with respect to the design variables of the powertrain components. Here we consider only the components of the two M/G units and the transmission. The framework can be expanded by including other components such as engine and battery. In regards to design variables of the M/G units, maximum speed and break-down torque are chosen to create the full-load characteristics by scaling empirical data from a base induction M/G. Geometric M/G design variables, such as stack length, element radii, the numbers of poles, phases, and coil turns, can be used to create efficiency maps as well as the full-load capacity maps, as in previous research [7]. These further considerations will be included in future research.

As detailed previously, the components' characteristics determine the constraints in the lower level problem. In this nested optimization sub-problem, the vehicle accelerates to 100 MPH, exerting the maximized output torque as in Fig. 12. (The specifications of the crossover SUV are provided in Table 3.) The acceleration performance should be less than 19 seconds, which is the constraint in the upper level problem. It is more common to use the 0-60 MPH acceleration performance; however, we chose 0-100 MPH to include the full-load performance in EVT2 mode at high velocities.

Table 3: Specifications of the crossover SUV

Engine	121 kW	Frontal area	3.12 m <sup>2</sup>
Battery	49 kW	Drag coefficient	0.37
Tire radius	0.358 m	Vehicle mass without M/Gs	1643 kg

The objective of the upper level problem is the cost for the M/G units. The change in overall costs due to the design variation in the planetary gear sets and final drive is neglected, but can be included with an appropriate

cost model. The M/G cost model which is based on geometric design variables [8] might produce more realistic results, along with the M/G characteristics model. In this stage of research, however, simpler cost models which use regression functions of M/G peak power were considered [9-11]. The cost and mass models are given in Equations (7) and (8):

$$C = 20 \times PP + 425 \quad (7)$$

$$M = 1.08 \times PP + 20 \quad (8)$$

where  $C$ ,  $M$ , and  $PP$  are the price (\$), mass (kg), and peak power (kW) of an induction motor, respectively.

## RESULTS

The eight-variable design space is fairly noisy due to the nested optimization sub-problem and the discontinuous nature of the shifting scheme. Rather than gradient-based search algorithms, we employed MADS (Mesh Adaptive Direct Search) to solve this problem with a highly non-smooth constraint function. The MADS is a pattern search algorithm like the Generalized Pattern Search (GPS), but allows local exploration in an asymptotically dense set of directions in the design space [12]. For the initial point, 500 design samples were generated using Latin Hypercube Sampling, and the best feasible solution was chosen. The optimization results are summarized in Table 4.

Table 4: Powertrain design optimization results

	Multi-mode	Multi-mode commonality	Single-mode
Transmission	PG1: 0.451 PG2: 0.611 PG3: 0.347 FD: 4.49	PG1: 0.389 PG2: 0.608 PG3: 0.389 FD: 4.49	PG: 0.354 FD: 4.43
M/G1	44.5 kW 7920 RPM 191 Nm	42.3 kW 8680 RPM 166 Nm	73.9 kW 12500 RPM 201 Nm
M/G2	30.3 kW 9690 RPM 106 Nm	42.3 kW 8680 RPM 166 Nm	153 kW 6500 RPM 804 Nm
0-100mph	19.0 sec.	19.0 sec	19.7 sec
0-60mph	6.7 sec.	6.6 sec.	7.0 sec.
M/G costs	\$ 2,340	\$ 2,540	\$ 5,370

For comparison, two additional powertrain design optimization cases were also investigated, and the results are presented in the last two columns of the table. In the second case, the multi-mode powertrain had two identical M/Gs. Thus, the problem was solved for six design variables instead of eight. The cost in the result does not include the commonality savings, and will have a lower value after including this benefit. In the third case, the powertrain used an input-split configuration, which had only one planetary gear set and no hydraulic clutch system. We assumed this difference

lead to 20 kg of mass reduction for this case. (For 10 kg of reduction, the optimal design has the M/G cost of \$ 5,490 and the 0-100mph acceleration of 19.84 seconds.) Since no feasible design seemed to be able to achieve less than 19 seconds of 0-100 MPH acceleration performance, 7 seconds of 0-60 MPH acceleration performance was used as the constraint instead. In both cases, the simulated vehicle had exactly the same specifications as in Table 3.

As noted in the introduction, the two-mode system resulted in significant improvements in dynamic performance at reduced cost of the M/G system. As can be seen in Fig. 11, the main contributor is the addition of FG1, which caused the difference between the two systems at low velocities in particular. The difference in costs are expected to become greater in reality because the cost model did not take into account the fact that high break-down torque motors are more expensive than high speed ones provided that they have the same peak power.

## CONCLUSION

As HEV technologies evolve, the development of integrated design frameworks that comprise all major powertrain components is of increasing importance. The paper used the three-dimensional operation space to find the optimal operation variables that produce the maximum powertrain output torque. We showed how the components' full-load characteristics affect the resultant system output and how the operation space is altered by using a different mode. Then, we integrated this procedure into a higher level optimization problem to evaluate the acceleration performance of M/G and transmission designs. The optimization results predicted the multi-mode system would have a better 0-60 MPH acceleration performance than a single-mode system, the latter having M/G costs more than twice higher.

Future work should seek to integrate more component models and geometric variables. Advanced optimization techniques, such as decomposition-based design, should also be considered to manage the expanded design space and noisy responses from nested optimization sub-problems.

## ACKNOWLEDGMENTS

This work was supported by the Korea Research Foundation Grant (KRF-2007-357-D00013) funded by the Korean Government (MEST) and the General Motors Collaborative Research Laboratory at the University of Michigan. The authors are also grateful to Dr. Sungtae Cho for his helpful comments. The opinions presented here are solely of the authors.

## REFERENCES

1. **Grewe, T., Conlon, B., and Holmes, A.** Defining the General Motors 2-mode hybrid transmission. *SAE paper 2007-01-0273*, 2007.
2. **Ahn, K., Cho, S., Lim, W., Park, Y., and Lee, J.** (2006). Performance analysis and parametric design of the dual-mode planetary gear powertrain. *Proc. IMechE, Part D: Journal of Automobile Engineering*, 220(11), 1601-1614.
3. **Schmidt, M., Klemen, D., Nitz, L., and Holmes, A.** "Two-Mode, Compound-Split, Hybrid Electro-Mechanical Transmission Having Four Fixed Gear Ratios", 2005, U.S. Pat. 6,953,409.
4. **Conlon, B.** Comparative analysis of single and combined hybrid electrically variable transmission operation modes. *SAE paper 2005-01-1162*, 2005.
5. **Ahn, K. and Cha, S.** Developing mode shift strategies for a two-mode hybrid powertrain with fixed gears. *SAE paper 2008-01-0307*, 2008.
6. **Benford, H. and Leising, M.** The lever analogy: A new tool in transmission analysis. *SAE paper 810102*, 1981.
7. **Allison, J.** *Optimal partitioning and coordination decisions in decomposition-based design optimization*. Ph.D. Thesis, Mechanical Engineering, University of Michigan, 2008.
8. **Simpson, T., Maier, J., and Mistree, F.** (2001) Product platform design: method and application. *Research in Engineering Design*, 13(1), 2-22.
9. **Cuenca, R., Gaines, L., and Vyas, A.** Evaluation of electric vehicle production and operating costs. *Argonne National Lab. technical report ANL/ESD-41*, 1999.
10. **Lipman, T. and Delucchi, M.** Hybrid electric vehicle design: Retail and lifecycle cost analysis. *ITS-Davis technical report UCD-ITS-RR-03-01*, 2003.
11. **Markel, T. and Simpson, A.** Cost-benefit analysis of plug-in hybrid electric vehicle technology. *National Renewable Energy Lab. technical report NREL/JA-540-40969*, 2006.
12. **Audet, C. and Dennis, J.** (2006) Mesh adaptive direct search algorithms for constrained optimization. *SIAM Journal on Optimization*, 17(1), 188-217.

## CONTACT

Kukhyun Ahn, Ph.D.

Postdoctoral Research Fellow, University of Michigan

kukhyun.ahn@gmail.com